Chinese Chemical Letters 33 (2022) 1267–1270

Contents lists available at ScienceDirect

Chinese Chemical Letters

journal homepage: www.elsevier.com/locate/cclet

Old commercialized magnetic particles new trick: Intrinsic internal standard

Chaoqun Wang[a], Ziqiang Deng[b], Hu Zhang[c], Rui Liu[b,*], Yi Lv[a]

[a] Analytical & Testing Center, Sichuan University, Chengdu 610064, China
[b] Key Laboratory of Green Chemistry and Technology of Ministry of Education, College of Chemistry, Sichuan University, Chengdu 610064, China
[c] Department of Gastroenterology, West China Hospital, Sichuan University, Chengdu 610041, China

ARTICLE INFO

Article history:
Received 12 May 2021
Revised 1 July 2021
Accepted 21 July 2021
Available online 29 July 2021

Keywords:
Magnetic particles
Ratiometric
Immunoassay
ICPMS
Carcinoembryonic antigen

ABSTRACT

Magnetic particles (MPs) are the most widely used commercialized engineering particles, which gained great success in various biological applications. Inspired by their intrinsic Fe isotope composition, we discovered a commercialized MPs-internal standard's novel function to realize the accurate quantification of biomolecules. The bioassay of carcinoembryonic antigen (CEA) was chosen as a modal system. The Fe isotope in MPs and Au isotope in report probes were simultaneously and sensitively detected by the elemental mass spectrometry. $^{197}Au/^{57}Fe$ isotopic ratios and CEA concentrations showed good linearity in the range of 0.6–300 ng/mL, with a detection limit of 0.09 ng/mL (3σ). The accuracy and precision of the proposed MPs-based immunoassay were greatly improved, by eliminating potential MPs loss during magnetic separation and absolute intensity fluctuations. Considering the exceptional availability and universality of commercialized MPs, the proposed method might open a new avenue for MPs' biological applications.

Magnetic particles (MPs) are typically composed of maghemite (gamma-Fe_2O_3) or magnetite (Fe_3O_4) with sizes ranging from nanometer to micrometer [1-4]. MPs demonstrated great successes in various biological applications, including cancer therapy, drug delivery, magnetic resonance imaging, blood purification, and molecular diagnosis [5-9]. For instance, Song *et al.* developed a sensitive near-infrared MPs imaging tracer with photothermal and magnetothermal properties [10], which was used for tumor ablation in mice. Bhatia *et al.* invented a highly sensitive iron-oxide nanoparticles-based tumor-penetrating protease biosensor to identify cancer lesions [11], which differentiated sub-5 mm lesions in human epithelial tumors and detected sub-2 mm nodules in the orthotopic model of ovarian cancer. Ingber *et al.* created MPs-based extracorporeal blood purification equipment for blood poisoning therapy [12], which be able to constantly wipe out pathogens and toxins from blood without identifying the infectious agent. The unique superparamagnetic property avoided labor- and time-consuming separation procedures such as centrifugation and chromatography, prompting the MPs-based method to be raised as the gold standard and rapidly commercialized in many aspects.

An ancient dream in the scientific community is the accurate quantification of biomolecules. To alleviate the signal fluctuation in bioassays, a general practice is the employment of internal standards (IS) [13-15]. IS could not only eliminate most accidental errors that happened during sample pretreatment but also make up for fluctuations in instrument monitoring [16,17]. Ideally, the internal standard's physio-chemical properties should be almost the same as that of the target analyte to effectively relieve matrix effects and signal fluctuations. Many research groups have devoted themselves to design the effective IS. For instance, Mercer *et al.* developed a series of DNA internal standards to form synthetic communities of artificial microbial genomes [18], which was validated in real metagenomic samples. Hunt *et al.* studied the two-dimensional infrared spectra of proteins in water [19], through the use of the solvent thermal response as an internal standard. Metal stable isotope tagging has recently emerged as an essential tool for the accurate detection of nucleic acid and protein biomarkers [20-29]. To realize isotopic ratiometry-based IS, Zhang *et al.* delicately introduced rare earth element isotope by bioprobes labeling [30,31], while Lim *et al.* successfully introduced metal isotopes by nanoparticles controllable synthesis [32-34]. Despite significant successes, the IS's wide application in bioassays is often hampered by sophisticated IS labeling or synthesis procedures.

* Corresponding author.
E-mail address: liur@scu.edu.cn (R. Liu).

https://doi.org/10.1016/j.cclet.2021.07.049
1001-8417/

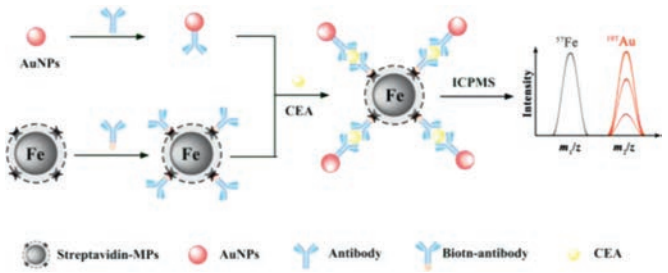

Fig. 1. Schematic diagram of the ratiometric immunoassay utilizing intrinsic Fe isotope in commercialized MPs as an IS.

Inspired by the above, we designed a novel ratiometric immunoassay utilizing intrinsic Fe isotope in commercialized MPs as an IS. The Fe isotope in MPs and Au isotope in bioprobes were sensitively and simultaneously detected by inductively coupled plasma mass spectrometry (ICPMS), which is regarded as one of the most potent commercialized tool for the quantification of metal elements and metal isotopes [35,36]. Carcinoembryonic antigen (CEA), a broad-spectrum biomarker for diseases including colorectal, lung, pancreatic, gastric, breast, ovarian cancers, was chosen as a model analyte [37,38]. The MPs were served as not only support and separator for immunoassay but also IS. The accuracy and reliability of the proposed MPs-based immunoassay were greatly enhanced by circumventing the challenge of MPs loss during magnetic separation and absolute intensity-related signal reading, which can bring about absolute signal intensity fluctuations. Considering the exceptional availability and universality of commercialized MPs, the proposed method might open a new avenue for MPs' biological applications.

The mechanism of the immunoreaction in this system is shown in Fig. 1. In this system, streptavidin-modified MPs are used as carriers, and gold nanoparticles are used as signal probes. First, Ab_1−MPs and Ab_2-AuNPs were synthesized by the specific reaction of streptavidin and biotin and the formation of Au-S bonds, respectively. Following that, the specific binding of antigens and antibodies enables MPs to successfully capture CEA antigens when Ab_1−MPs solutions and CEA samples were added to the system. Next, antibodies (Ab_2) on the AuNPs surface identify CEA and form MPs-CEA-AuNPs complexes when Ab_2-AuNPs were added to the acquired MPs-CEA solution. Unreacted AuNPs were removed by magnetic separation. The ICPMS signal value of AuNPs in the final solution is positively correlated with the CEA concentration in the sample to a certain extent. Unfortunately, the MPs are easily lost during the magnetic separation, resulting in reduced accuracy, which significantly hinders the method's widespread application. To improve the accuracy of the proposed method, the ^{57}Fe isotope in MPs and ^{197}Au isotope in bioprobes were simultaneously detected by high-resolution ICPMS, and the relationship between the ^{197}Au/^{57}Fe value and the CEA concentration was investigated. The accuracy and reliability of the proposed MPs-based ratiometric immunoassay were greatly enhanced by eliminating potential MPs loss during magnetic separation and correcting the deviation measuring of high-resolution ICPMS.

Figs. 2a and b exhibit the TEM images of the MPs and the MPs-CEA-AuNPs complex formed by the immunoreaction, respectively. Comparing the two, there are many small-sized particles in Fig. 2b, and the size of these particles is consistent with the AuNPs (Fig. S1 in Supporting information). The particle size was characterized by TEM, and the average size is around 12 nm for AuNPs, and 2.8 μm for MPs. Moreover, comparing the EDS spectrum before (Fig. S4a in Supporting information) and after (Fig. S4b in Supporting information) the immunoreaction, the Au element's peak appears in the latter spectrum. The clear distribution of Au elements on MPs is

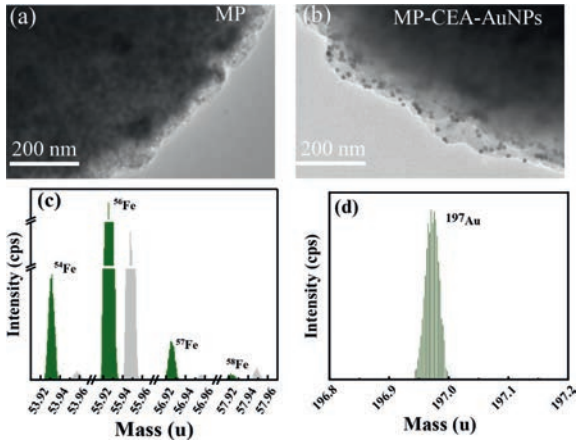

Fig. 2. (a) TEM images of MPs. (b) TEM images of MPs-CEA-AuNPs. (c) The interference of ^{54}Fe, ^{56}Fe,^{57}Fe and ^{58}Fe in the mass range of 53.91–53.97, 55.91–55.97, 56.91–56.97, 57.91–57.97, respectively. Green, signal peak; gray, interference peak. (d) The interference of ^{197}Au in the mass range of 196.8–197.2.

shown in the EDS element mapping image of Au, Fe, and O (Fig. S5 in Supporting information). These phenomena reveal the successful immunoreaction occurrence, and the Ab_1−MPs, antigen, and Ab_2-AuNPs form a sandwich-type structure (MPs-CEA-AuNPs).

To investigate whether the Fe isotopes in the selected commercial MPs were sufficiently uniform to be used as internal standard elements. Since the abundance of ^{58}Fe is low (0.28%), and ^{56}Fe is interfered with by ^{40}Ar^{16}O and ^{40}Ca^{16}O, the ^{54}Fe and ^{57}Fe were investigated in this section (Fig. 2c). Different volumes of MPs solutions were digested under the same conditions, and then the signal values of the ^{54}Fe and ^{57}Fe isotopes were detected using high-resolution inorganic mass spectrometry. The good linear correlation between the intensity of ^{54}Fe, ^{57}Fe and volume is shown in Fig. S6 (Supporting information). Since the better stability of ^{57}Fe, the signal value of ^{57}Fe is used as the internal standard in this experiment.

Further, we investigated the interference of ^{57}Fe and ^{197}Au when using high-resolution inorganic mass spectrometry to acquire their signal value. The signal value of the mass-to-charge ratio in the range of 56.91–56.97 was investigated (Fig. 2c). There is an interference peak with a mass-to-charge ratio of 56.96, which is attributed to ArOH. The ArOH peak and ^{57}Fe peak are wholly separated, and their resolution is more than 4000, which means that ^{57}Fe can be detected without ArOH interference. The signal value of the mass-to-charge ratio in the range of 196.8–197.2 was observed, and no interference peak appeared in Fig. 2d. Therefore, it is feasible to employ ^{57}Fe as an internal standard and ^{197}Au as a signal probe.

In order to obtain better performance of the proposed ratiometric immunoassay, we have optimized the experimental parameters, which include the amount of reagent and reaction time.

The dilution factor of the Ab_2-AuNPs solution is closely related to non-specific adsorption and reaction efficiency. Therefore, under the same experimental conditions, this method's analytical performance under different dilution ratios of Ab_2-AuNPs was discussed. A smaller dilution factor means that the concentration of Ab_2-AuNPs solution in the system is very high, and the non-specific adsorption of AuNPs leads to high blank intensity, resulting in smaller S/N values. The higher the dilution factor, the lower the concentration of Ab_2-AuNPs in the system, and the smaller S/N values were observed in Fig. S7 (Supporting information), which could be attributed to the lower collision efficiency between AuNPs and target antigen. The results demonstrate that the system has a highest S/N value when the dilution ratio of Ab_2-AuNPs solution is 5. There-

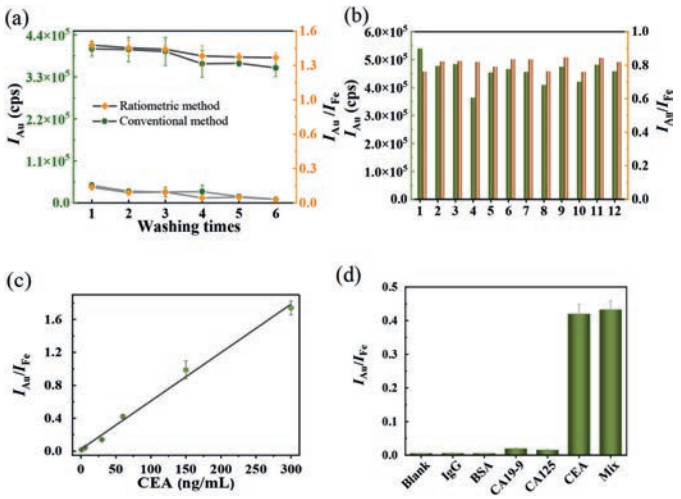

Fig. 3. (a) The signal values of blanks and samples obtained by traditional immunoassay and the proposed ratiometric immunoassay at different washing times. (b) The corresponding I_{Au}/I_{Fe} and I_{Au} values of the 12 samples at the same CEA concentration. (c) Calibration curves between the I_{Au}/I_{Fe} and CEA concentration. *I* represent the intensity value of ICPMS. (d) The I_{Au}/I_{Fe} values of 100 ng/mL IgG, 100 ng/mL BSA, 100 U/mL CA19–9, 100 U/mL CA125, 100 ng/mL CEA and mixture.

fore, the dilution ratio of Ab_2-AuNPs solution is 5 in this experiment.

Since the incubation time between antigens and antibodies is an essential parameter of the system, it is necessary to optimize the incubation time for better analytical performance of the proposed ratiometric immunoassay. Fig. S8 (Supporting information) displays the influence of the incubation time of Ab_1−MPs solution and antigens on the S/N value. With the increase in the incubation time between Ab_1−MPs and antigen from 30 min to 60 min, the S/N value increased gradually, and the S/N value presented a platform when the incubation time exceeds 60 min, indicating that the reaction between Ab_1−MPs and CEA was basically completed at 60 min. Considering the analytical performance and time consumption, 60 min was selected to incubate Ab_1−MPs and CEA in the following experiments.

In addition, the appropriate loading amounts of antibodies on AuNPs, the volume of MPs solution, and the incubation time of Ab_2-AuNPs binding to antigen were also studied. As shown in Figs. S9-S11 (Supporting information), the optimal conditions were 13 μg, 2 μL and 60 min, respectively.

To investigate whether the proposed ratiometric immunoassay successfully corrected the reduced accuracy caused by MPs loss during washing. The intensity of Au and the value of Au/Fe were observed at various washing times (Fig. 3a). Comparing traditional immunoassay and the proposed ratiometric immunoassay, the value of Au and Au/Fe exhibited a significant downward trend in the first four washes, which was attributed to the release of non-specifically adsorbed AuNPs from the MPs surface. The ratiometric immunoassay possessed better stability than the traditional immunoassay when the washing exceeds four times. These phenomena implied that the proposed ratiometric immunoassay has successfully corrected the loss of MPs to some extent, and that more accurate signal values can be obtained in this experiment. Taking into account the non-specific adsorption of AuNPs and the loss of MPs caused by washing, the MPs-CEA-AuNPs complex was washed four times in this experiment.

Furthermore, to discuss whether the accuracy of the immunoassay was improved by ratiometric analysis, the signal values of 12 samples with the same CEA concentration obtained by traditional immunoassay and the proposed ratiometric immunoassay were compared. The corresponding I_{Au} value and I_{Au}/I_{Fe} value are shown in Fig. 3b, respectively. The relative standard deviations of I_{Au}/I_{Fe} and I_{Au} are 3.8% and 9.2%, respectively, implying higher stability and precision of the data obtained by ratiometric immunoassay.

Table 1
Analytical results for the determination of CEA in real samples.

Sample	ELISA		The proposed immunoassay	
	CEA (ng/mL)	RSD (%)	CEA (ng/mL)	RSD (%)
1	14.40	7.7	15.68	4.1
2	4.11	3.3	4.62	1.2
3	5.39	5.4	6.37	3.9
4	26.96	3.5	28.07	1.5
5	49.35	5.2	50.19	3.5

Under optimal conditions, the relationship between I_{Au}/I_{Fe} and CEA concentrations was investigated. As the CEA concentration increased from 0.6 ng/mL to 300 ng/mL, the ICPMS intensity of ^{197}Au increased (Fig. S13a in Supporting information), while the ICPMS intensity of ^{57}Fe almost remained unchanged (Fig. S13b in Supporting information). As revealed in Fig. 3c, I_{Au}/I_{Fe} and CEA concentration have a good linear relationship in the range of 0.6–300 ng/mL. The calibration curves equation is $I_{Au}/I_{Fe} = 5.874 \times 10^{-3}C + 0.023$, with the correlation coefficient $R = 0.997$, where *I* represent the intensity value of ICPMS at medium resolution mode and *C* represent the concentration of CEA. The detection limit is 0.09 ng/mL (3SD/*k*, SD is the standard deviation of 10 blank samples).

The interference detection of a series of antigens was utilized to test the platform's specificity to the target. Immunoglobulin G (IgG) and bovine serum albumin (BSA) are often used in bioanalytical research, and BSA is the blocking agent in this experiment. Carbohydrate antigen 19–9 (CA19–9) and carbohydrate antigen 125 (CA125) are two tumor markers that can be secreted by the same cancer cells as CEA. Fig. 3d shows the effect of 100 ng/mL IgG, 100 ng/ml BSA, 100 U/mL CA19–9, 100 U/mL CA125, 100 ng/mL CEA and mixture sample on I_{Au}/I_{Fe} values. The final concentration of five antigens in the mixture sample was the same as that of the former. IgG and BSA samples' values were basically consistent with the blank values, and the values of CA19–9 and CA125 samples were slightly higher than the blank values, while the values of CEA were much higher than other antigens. The CA19–9 and CA125 samples' values were slightly higher than those of the blank, which could be attributed to the two antigens possibly containing CEA impurities caused by incomplete purification during the preparation process. In addition, the values of the mixture samples were nearly consistent with those of CEA, suggesting that these antigens would not interfere with CEA detection in this experiment.

Furthermore, the proposed ratiometric immunoassay was applied to detect CEA in 5 clinical serum specimens. The obtained results were compared with those of commercially available ELISA as a reference method. As shown in Table 1, the relative standard deviation (RSD) was 1.2%−4.1%. No significant differences were encountered, implying that the proposed ratiometric immunoassay has the potential for clinical application.

In conclusion, inspired by magnetic particles' intrinsic Fe isotope composition, we exploited a novel function of MPs-internal standard and constructed a novel simple ratiometric immunoassay based on high-resolution ICPMS. Based on the novel MPs-internal standard system, a sandwich-type ratiometric immunoassay was established to detect CEA selected as the model analyte. The ratio value ($^{197}Au/^{57}Fe$) instead of a single Au isotope signal can eliminate potential MPs loss during magnetic separation and absolute intensity fluctuations, and improve the accuracy and precision of the proposed MPs-based immunoassay. Considering the exceptional availability and universality of commercialized MPs, the

proposed method might open a new avenue for MPs' biological applications.

Declaration of competing interest

The authors report no declarations of interest.

Acknowledgments

This work is supported by the National Natural Science Foundation of China (Nos. 22074096 and 22074098), Talents Program of Sichuan Province (No. 903), 1.3.5 Project for Disciplines of Excellence of West China Hospital, Sichuan University (No. ZYJC18037), and the Fundamental Research Funds for the Central Universities (No. 20826041D4117). The Chengdu 7th People's Hospital is gratefully thanked for supplying serum samples. Dr. Peng Wu and Dr. Jing Hu from the Analytical & Testing Center, Sichuan University, and Dr. Chunxia Wang from the College of Chemistry, Sichuan University, are gratefully thanked for their helpful discussion or/and technical assistance.

Supplementary materials

Supplementary material associated with this article can be found, in the online version, at doi:10.1016/j.cclet.2021.07.049.

References

[1] M.K. Masud, J. Na, M. Younus, et al., Chem. Soc. Rev. 48 (2019) 5717–5751.
[2] C. Liu, S.F. Wu, Y.B. Yan, et al., TrAC-Trends Anal. Chem. 121 (2019) 10.
[3] H. Gu, K. Xu, C. Xu, B. Xu, Chem. Commun. (2006) 941–949.
[4] L. Zhou, X. Zhang, L. Liu, Y. Wei, J. Yuan, Chin. J. Chem. 35 (2017) 977–983.
[5] S.E. Kim, M.V. Tieu, S.Y. Hwang, M.H. Lee, Micromachines 11 (2020) 20.
[6] M. Colombo, S. Carregal-Romero, M.F. Casula, et al., Chem. Soc. Rev. 41 (2012) 4306–4334.
[7] Y. Guo, Y. Wang, S. Li, et al., Chem. Commun. 53 (2017) 4826–4829.
[8] Q. Bi, X. Song, A. Hu, et al., Chin. Chem. Lett. 31 (2020) 3041–3046.
[9] G. Ma, H. Yue, Chin. J. Chem. 38 (2020) 911–923.
[10] G.S. Song, M. Kenney, Y.S. Chen, et al., Nat. Biomed. Eng. 4 (2020) 325.
[11] E.J. Kwon, J.S. Dudani, S.N. Bhatia, Nat. Biomed. Eng. 1 (2017) 0054.
[12] J.H. Kang, M. Super, C.W. Yung, et al., Nat. Med. 20 (2014) 1211–1216.
[13] C. Wang, R. Liu, J. Hu, Y. Lv, Chem. Eur. J. 25 (2019) 12270–12274.
[14] H. Zhao, J. Li, X. Ma, et al., Chin. Chem. Lett. 29 (2018) 102–106.
[15] H. Xiao, P. Liu, S. Zheng, et al., Chin. Chem. Lett. 31 (2020) 2423–2427.
[16] W. Shen, X. Lin, C.Y. Jiang, et al., Angew. Chem. Int. Ed. 54 (2015) 7308–7312.
[17] S. Goggins, C. Naz, B.J. Marsh, C.G. Frost, Chem. Commun. 51 (2015) 561–564.
[18] S.A. Hardwick, W.Y. Chen, T. Wong, et al., Nat. Commun. 9 (2018) 10.
[19] S. Hume, G.M. Greetham, P.M. Donaldson, et al., Anal. Chem. 92 (2020) 3463–3469.
[20] R. Liu, S. Zhang, C. Wei, et al., Acc. Chem. Res. 49 (2016) 775–783.
[21] C. Ji, Y. Liang, F. Ge, L. Yang, Q. Wang, Anal. Chem. 91 (2019) 7032–7038.
[22] X. Liu, S.Q. Zhang, Z.H. Cheng, et al., Anal. Chem. 90 (2018) 12116–12122.
[23] B.-.R. Li, H. Tang, R.Q. Yu, J.-.H. Jiang, Anal. Chem. 92 (2020) 2379–2382.
[24] G.Y. Xiao, B.B. Chen, M. He, B. Hu, Anal. Chim. Acta 1096 (2020) 18–25.
[25] Y.P. Cao, G.C. Mo, J.S. Feng, et al., Anal. Chim. Acta 1028 (2018) 22–31.
[26] M. Wang, L.N. Zheng, B. Wang, et al., Anal. Chem. 86 (2014) 10252–10256.
[27] S.D. Tanner, D.R. Bandura, O. Ornatsky, et al., Pure Appl. Chem. 80 (2008) 2627–2641.
[28] Z. Hu, G.W. Sun, W.C. Jiang, et al., Anal. Chem. 91 (2019) 5980–5986.
[29] Q. Zhao, X.F. Lu, C.G. Yuan, X.F. Li, X.C. Le, Anal. Chem. 81 (2009) 7484–7489.
[30] G. Sun, Y. Zhang, Y. Zhang, et al., Talanta 189 (2018) 249–253.
[31] G.J. Han, S.C. Zhang, Z. Xing, X.R. Zhang, Angew. Chem. Int. Ed. 52 (2013) 1466–1471.
[32] J. Ko, H.B. Lim, Anal. Chem. 86 (2014) 4140–4144.
[33] H.W. Choi, K.H. Lee, N.H. Hur, H.B. Lim, Anal. Chim. Acta 847 (2014) 10–15.
[34] H. Jang, H.B. Lim, Bull. Korean Chem. Soc. 37 (2016) 1433–1439.
[35] X. Lin, W. Guo, L.L. Jin, S.H. Hu, Atom. Spectrosc. 41 (2020) 1–10.
[36] J.H. Liu, L.N. Zheng, J.W. Shi, et al., Atom. Spectrosc. 42 (2021) 114–119.
[37] H.R. Tang, H. Wang, C. Yang, et al., Anal. Chem. 92 (2020) 3042–3049.
[38] M.Q. He, K. Wang, W.J. Wang, Y.L. Yu, J.H. Wang, Anal. Chem. 89 (2017) 9292–9298.